# New supramolecular isomers with 2D $4^4$ square-grid and 3D $6^5{\cdot}8$ frameworks in a one-pot synthesis; reversible solvent uptake and intriguing luminescence properties†

**Chih-Chieh Wang,*[a] Wei-Zeng Lin,[a] Wei-Ting Huang,[a] Mei-Ju Ko,[a] Gene-Hsiang Lee,[b] Mei-Lin Ho,[b] Chun-Wei Lin,[b] Chun-Wei Shih[b] and Pi-Tai Chou*[b]**

*Received (in Cambridge, UK) 1st November 2007, Accepted 4th January 2008*
*First published as an Advance Article on the web 23rd January 2008*
**DOI: 10.1039/b716953a**

**Two supramolecular isomers of $[Ni(4\text{-bpd})_2(NCS)_2]$ (4-bpd = 1,4-bis(4-pyridyl)-2,3-diaza-1,3-butadiene) with 2D $4^4$ square-grid and 3D $6^5{\cdot}8$ frameworks are co-crystallized in a one-pot reaction, both of which exhibit interesting luminescence properties and reversible adsorption–desorption with respect to guest solvents.**

Supramolecular isomers[1] in coordination polymers have received much attention, mainly due to their structural diversity and hence their topologies. These are governed by either specific building units[1,2] or other perturbation factors, such as the conformational flexibility of ligands,[1c] and the influence of guests and solvents. Among these factors, the effect of solvent has been demonstrated in numerous examples,[1,2] in which different coordination polymer species could be selectively afforded from the same components using different solvents. Frameworks based solely upon square-planar nodes can have several topologies: the 2D $4^4$ square-grid,[3] the 3D $6^4{\cdot}8^2$ NbO,[4] the $6^5{\cdot}8$ $CdSO_4$,[5] the "dense" $7^5{\cdot}9$ [6] and the unusual $4^2{\cdot}8^4$.[7] However, only few exquisite examples have been reported of supramolecular isomers based on square-planar nodes.[2] For instance, in the self-assembled "$Cu(Pyac)_2$" framework with a square-planar node, two structural topologies of 2D $4^4$ square-grid and 3D $6^4{\cdot}8^2$ NbO are crystallized separately from different solvents.[2a] Another example of supramolecular isomerism is the coordination polymer of $[Zn(nicotinate)_2]$, possessing 2D $4^4$ and unusual $4^2{\cdot}8^4$ topologies under different solvent systems.[2c] Evidently, new supramolecular isomers among these topologies are emergent and worth further exploration.

In this contribution, we conduct the synthesis of supramolecule $[Ni(4\text{-bpd})_2(NCS)_2]$ (4-bpd = 1,4-bis(4-pyridyl)-2,3-diaza-1,3-butadiene) with a square-planar node (see Fig. 1), and report the first prototype of 2D $4^4$ square-grid and 3D $6^5{\cdot}8$ frameworks co-crystallized in a facile one-pot reaction. The variation in structural topology results from the conformational freedom of the 4-bpd[8] ligand through rotation of the diaza group R–C═N–N═C–R (Fig. 1), which renders upon them intriguingly different luminescence properties, spatially resolved by confocal microscopy. Both isomers possess reversible solvent ($EtOH/H_2O$) uptake properties, making them suitable for gas molecule storage.

The reaction of $NiCl_2{\cdot}6H_2O$ with KSCN and 4-bpd in a 1 : 1 : 1 molar ratio in $H_2O$/EtOH (1 : 1) solution leads to the formation of two kinds of crystal with distinct differences in color, purple and light-yellow. As revealed by X-ray single-crystal analyses, the structures of the purple and light-yellow crystals are ascribed to supramolecular isomers, namely $[Ni(4\text{-bpd})_2(NCS)_2]{\cdot}3(EtOH){\cdot}(H_2O)$ (**1**) and $[Ni(4\text{-bpd})_2(NCS)_2]{\cdot}(EtOH){\cdot}(H_2O)$ (**2**), respectively (see Fig. S1 for ORTEP views†).[9] For both compounds **1** and **2**, statically-identical hexacoordinate environments are found at the $Ni^{II}$ centers, which are bonded to two $NCS^-$ and four 4-bpd ligands. Four 4-bpd ligands form a square-planar arrangement at the metal center as the basic building unit for constructing their metal–organic frameworks. As shown in Fig. 2(a), compound **1** reveals a two-dimensional $4^4$ square-grid framework with a grid size of 15 × 15 Å. Adjacent independent layers are then arranged in an orderly manner as ABAB-alternating stacking patterns, creating 1D channels, in which solvent (guest)

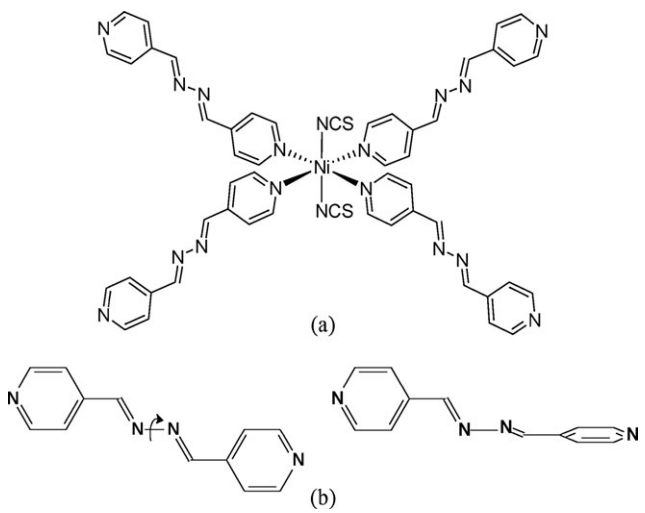


**Fig. 1** (a) Square-planar node of $[Ni(4\text{-bpd})_2(NCS)_2]$. (b) The conformation flexibility of 4-bpd, with the dihedral angle of diaza group R–C═N–N═C–R for **2** (180°, left) and **1** (90°, right).

[a] *Department of Chemistry, Soochow University, Taipei 111, Taiwan. E-mail: ccwang@scu.edu.tw; Tel: +886 (2) 2881 9471 ext. 6824*
[b] *Department of Chemistry, National Taiwan University, Taipei 106, Taiwan. E-mail: chop@ntu.edu.tw; Fax: +886 (2) 2369 5208; Tel: +886 (2) 3366 3894*

† Electronic supplementary information (ESI) available: Synthetic methods, ORTEP views, and further experimental and crystal structure data. See DOI: 10.1039/b716953a

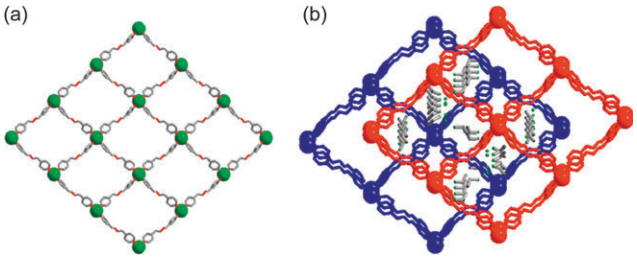


**Fig. 2** 2D square-grid framework of $[Ni(4\text{-bpd})_2(NCS)_2]\cdot 3(EtOH)\cdot(H_2O)$ (**1**). (a) View of one square-grid layer. The Ni atoms are shown in green; the $NCS^-$ and solvent (ethanol and water) molecules are omitted for clarity. (b) The ABAB stacking pattern of four layers (red and blue), showing the orientations of the 1D channels filled by EtOH and $H_2O$ guest aggregates.

molecules, such as ethanol and water, form hydrogen-bonded aggregates (Fig. 2(b)). The Ni–Ni separations through the 4-bpd bridges are 15.44 and 15.51 Å, and the nearest interlayer Ni–Ni distance is 8.93 Å. In sharp contrast, compound **2** reveals a 3D $6^5\cdot 8$ framework, as shown in Fig. 3(a). The much larger intra-framework spaces are occupied by two other identical but independent networks, which interpenetrate the first and each other, as shown in the schematic representation of Fig. 3(b). The Ni–Ni separations through the 4-bpd bridges are in the range 15.52–15.54 Å, and the nearest inter-framework Ni–Ni distance is 9.12 Å. Despite this interpenetration, compound **2** also retains 1D channels, which are filled with aggregated solvent molecules (ethanol and water) (Fig. 3(c)).

With the same chemical formula and solvent system, the factor that governs the choice of topology is thus of great interest. More careful examination indicates that the most salient feature of the structural differences between **1** and **2** lies in the conformational freedom, through single bond rotation of the diaza group R–C═N–N═C–R, of the 4-bpd ligand. In **1**, the dihedral angles between the two aza groups are 89.4(5) and 105.4(5)° (right-hand structure in Fig. 1(b)), while in sharp contrast, the dihedral angles between two aza groups are 180 and 148.0(8)° in **2** (left-hand structure in Fig. 1(b)). Such conformational flexibility of the 4-bpd ligand may account for the supramolecular isomerism of **1** and **2** with different MOFs. To the best of our knowledge, no similar type of isomerism has been previously reported. Moreover, desolvated TGA analyses[10] reveal that their 2D (**1**) and 3D (**2**) frameworks are thermally stable up to 160 and 190 °C, respectively. In particular, the TGA studies revealed that the guest ethanol solvents in the pores of **1** and **2** could be desorbed by heating them to 120 and 140 °C, respectively, and re-adsorbed by exposing the material to ethanol vapour upon cooling to room temperature. These procedures were repeated for several cycles to establish the reversibility of the process (see Fig. 4 and Fig. S2†).

The different colors of the crystals, viewed with the naked eye, implies that the electronic transition should be subject to the structural variation, particularly of the diaza group R–C═N–N═C–R in different configurations (*vide supra*), in combination with the associated structural topologies. In solution (THF), the characteristic absorption band for complexes **1** and **2** at ~290 nm can reasonably be assigned to an $S_0 \rightarrow S_1$ ($\pi$–$\pi^*$) transition of the 4-bpd ligand due to its resemblance as a spectral feature to free 4-bpd. Fig. 5 also depicts the emission spectra of complexes **1** and **2** as single-crystals acquired using a confocal microscope at room temperature. The corresponding photophysical data are listed in Table 1. For both crystals, the confocal images (~10–12 μm in diameter) used to acquire the emission spectra are also shown in the inset of Fig. 5. Clearly, **1** and **2** exhibit green-yellow

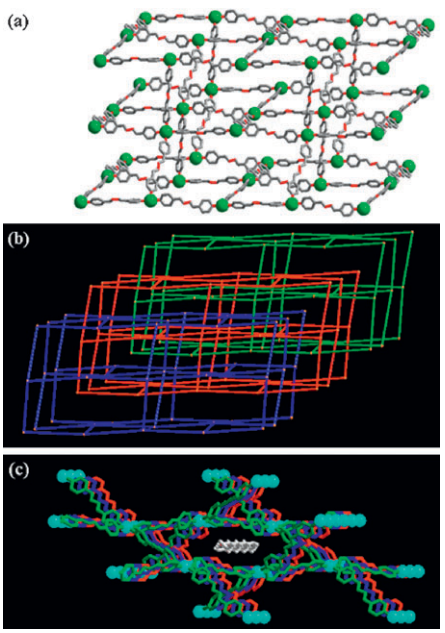


**Fig. 3** (a) 3D $6^5\cdot 8$ $CdSO_4$ framework, (b) schematic representation of the triple interpenetration and (c) 1D channel in the 3D triply-interpenetrated $CdSO_4$ framework of $[Ni(4\text{-bpd})_2(NCS)_2]\cdot(EtOH)\cdot(H_2O)$ (**2**). Note, for clarity in (a), the NCS and solvent (ethanol and water) molecules are omitted.

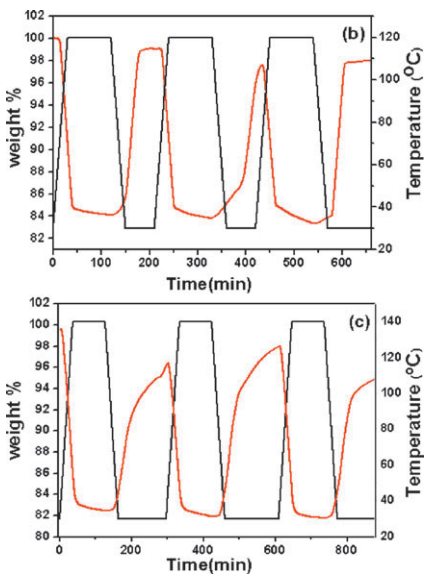


**Fig. 4** (a) The TGA measurements of cyclic ethanol desorption and absorption processes for **1** were repeated three times. (b) The TGA measurements of cyclic ethanol desorption and absorption processes for **2** were repeated three times. The variation of weight loss with time is shown as a red line. The variation of temperature with time is shown as a black line.

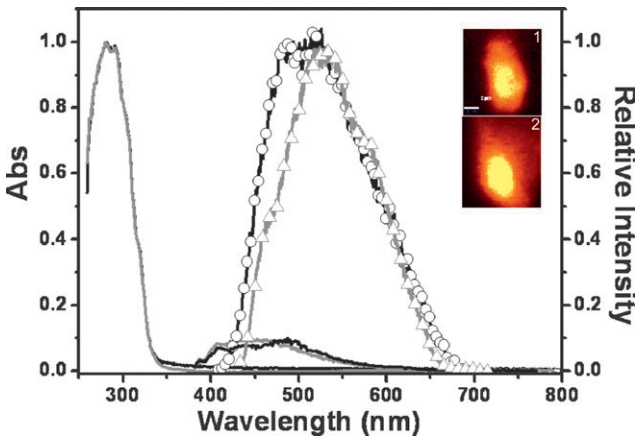


**Fig. 5** The absorption and emission spectra of **1** (black) and **2** (grey) in THF. The emission of **1** (□) and **2** (△) in single-crystals. Inset: Confocal images of complexes **1** and **2**. The scale bar is 3 μm.

**Table 1** Photophysical properties of complexes **1** and **2**

| | $\lambda_{max}$/nm[a] | $\lambda_{max}$/nm[b] | $\tau_{obs}$/ps[c] |
|---|---|---|---|
| **1** | 478 | 505 | 210 |
| **2** | 475 | 528 | 63 |

[a] Emission was detected in THF ($\sim 1.2 \times 10^{-5}$ M) at 298 K. [b] Emission was detected in a single-crystal at 298 K. [c] Lifetimes were detected in single-crystals. Note: Lifetimes for both **1** and **2** in THF were beyond the system limit of 50 ps.

emission, with peak wavelengths at 505 and 528 nm, respectively. Since the same emission spectra were obtained throughout the different probing areas of the crystals, the possibility that the resulting emission originates from crystal defects can be discarded. Accordingly, the spectral differences between **1** and **2** in single-crystals are intrinsic, and could plausibly be due to the aforementioned structural variation. The red shift of emission in **2** can tentatively be rationalized by its tighter molecular packing (see Fig. 3(c)) than in **1**. Indirect support of this viewpoint is rendered by the higher TGA depicted in Fig. S2,† in which **2** has a higher TG (190 °C) than **1** (160 °C). In a qualitative manner, these features of the molecular arrangement may be reminiscent of a J-aggregate-like configuration for **2**. In contrast, such interactions are greatly reduced in **1** due to the alternating slab arrangement (Fig. 2(b)). This viewpoint is also supported by the great difference in the observed lifetime ($\tau_{obs}$) of 210 and 63 ps for **1** and **2**, respectively (see Table 1). Upon dissolution in ethanol/water, both **1** and **2** exhibit very weak but nearly identical emission spectra maximized at ~475 nm. This, in combination with the same absorption spectral features (Fig. 5), implies that the topologies of **1** (2D) and **2** (3D) may have collapsed in solution.

In summary, based on a facile one-pot synthetic route, we have demonstrated for the first time the versatility of 4-bpd bridges for building up a new type of supramolecular isomer with 2D $4^4$ square-grid and 3D $6^5{\cdot}8$ frameworks. While the configuration of 4-bpd (see Fig. 1) seems to govern the dimensions of the frameworks, the hydrogen-bonded aggregates among the guest solvent molecules play important roles in stabilizing the pores of both MOFs. For both **1** and **2**, the thermally stable properties of the structures and the reversible adsorption–desorption process with respect to the guest solvents may find potential applications in gas molecule storage.[12] These new topology isomers, made in a one-pot reaction, may spark a broad spectrum of interest in the field of supramolecular chemistry.

## Notes and references


1 (*a*) M. J. Zaworotko, *Chem. Commun.*, 2001, 1 and references therein; (*b*) B. Moulton and M. J. Zaworotko, *Chem. Rev.*, 2001, **101**, 1629 and references therein; (*c*) T. L. Hennigar, D. C. MacQuarrie, P. Losier, R. D. Rogers and M. J. Zaworotko, *Angew. Chem., Int. Ed. Engl.*, 1997, **36**, 972.

2 (*a*) B. Chen, F. R. Fronczek and A. W. Maverick, *Chem. Commun.*, 2003, 2166; (*b*) I. S. Lee, D. M. Shin and Y. K. Chung, *Chem.–Eur. J.*, 2004, **10**, 3158; (*c*) B. Rather, B. Moulton, R. D. B. Walsh and M. J. Zaworotko, *Chem. Commun.*, 2002, 694.

3 M. Fujita, Y. J. Kwon, S. Washizu and K. Ogura, *J. Am. Chem. Soc.*, 1994, **116**, 1151.

4 (*a*) T. Niu, X. Wang and A. J. Jacobson, *Angew. Chem., Int. Ed.*, 1999, **38**, 1934; (*b*) M. Eddaoudi, J. Kim, M. O'Keeffe and O. M. Yaghi, *J. Am. Chem. Soc.*, 2002, **124**, 376.

5 L. Carlucci, N. Cozzi, G. Ciani, M. Moret, D. M. Proserpio and S. Rizzato, *Chem. Commun.*, 2002, 1354.

6 (*a*) K. N. Power, T. L. Hennigar and M. J. Zaworotko, *Chem. Commun.*, 1998, 595; (*b*) M. J. M. J. Plater, M. R. St. J. Foreman and J. M. S. Skakle, *Cryst. Eng.*, 2001, **4**, 319.

7 L. L. Carlucci, G. Ciani, P. Macchi and D. M. Proserpio, *Chem. Commun.*, 1998, 1837.

8 (*a*) Y.-B. Dong, M. D. Smith, R. C. Layland and H.-C. zur Loye, *Chem. Mater.*, 2000, **12**, 1156; (*b*) D. M. Ciurtin, Y.-B. Dong, M. D. Smith, T. Barclay and H.-C. zur Loye, *Inorg. Chem.*, 2001, **40**, 2825; (*c*) G. Zhang, G. Yang and J. S. Ma, *Cryst. Growth Des.*, 2006, **6**, 1897.

9 Crystal data for **1**: $C_{32}H_{40}N_{10}NiO_4S_2$, $M_r$ = 751.57, monoclinic, space group $P2_1/c$, $a$ = 22.5500(4), $b$ = 18.8168(3), $c$ = 8.7610(2) Å, $\beta$ = 92.6734(9)°, $V$ = 3713.4(1) Å$^3$, $Z$ = 4, $\mu$ = 0.684 mm$^{-1}$, $\rho_{calc}$ = 1.344 g cm$^{-3}$, $T$ = 150(2) K, GOF = 1.074, R1 (w$R2$) = 0.0690 (0.2063) [5908 observed ($I > 2\sigma(I)$)] for 8492 ($R_{int}$ = 0.0381) independent reflections out of a total of 20076 reflections with 449 parameters. CCDC 666607. Crystal data for **2**: $C_{28}H_{28}N_{10}NiO_2S_2$, $M_r$ = 659.43, monoclinic, space group $P2_1/c$, $a$ = 13.8640(5), $b$ = 13.8737(5), $c$ = 21.1162(8) Å, $\beta$ = 102.531(1)°, $V$ = 3964.8(3) Å$^3$, $Z$ = 4, $\mu$ = 0.629 mm$^{-1}$, $\rho_{calc}$ = 1.105 g cm$^{-3}$, $T$ = 220(2) K, GOF = 1.089, R1 (w$R2$) = 0.0952 (0.2827) [5429 observed ($I > 2\sigma(I)$)] for 6985 ($R_{int}$ = 0.0448) independent reflections out of a total of 31705 reflections with 386 parameters. CCDC 666608. Data collection was performed on a Bruker SMART ApexCCD diffractometer with graphite-monochromated Mo-$K_\alpha$ radiation. The structure was solved by direct methods using the SHELXTL program[11] and extended using Fourier techniques. For crystallographic data in CIF or other electronic format, see DOI: 10.1039/b716953a.

10 Before making TGA measurements, samples of both **1** and **2** were placed in an oven at 120 °C for several hours to remove the guest solvents.

11 *SHELXTL 5.03 (PC Version): Program Library for Structure Solution and Molecular Graphics*, Siemens Analytical Instruments Division, Madison, WI, 1995.

12 (*a*) N. L. Rosi, J. Eckert, M. Eddaoudi, D. T. Vodak, J. Kim, M. O'Keeffe and O. M. Yaghi, *Science*, 2003, **300**, 1127 and references therein; (*b*) R. Matsuda, R. Kitaura, S. Kitagawa, Y. Kubota, R. V. Belosludov, T. C. Kobayashi, H. Sakamoto, T. Chiba, M. Takata, Y. Kawazoe and Y. Mita, *Nature*, 2005, **436**, 238.